# Design of a 4-Seat, General Aviation, Electric Aircraft

Arvindhakshan Rajagopalan Srilatha
Aerospace Engineering
San Jose State University
San Jose, California, USA
arvindhakshan.rs@gmail.com

Nikos J. Mourtos
Aerospace Engineering
San Jose State University
San Jose, California, USA
nikos.mourtos@sjsu.edu

*Abstract* — **Range and payload of current electric aircraft has been limited primarily due to low energy density of batteries. However, recent advances in battery technology promise storage of more than 1 kWh of energy per kilogram of weight in the near future. This kind of energy storage makes possible the design of an electric aircraft comparable, if not better, to existing state-of-the art general aviation aircraft powered by internal combustion engines. The paper explores through parametric studies the effect of lift-to-drag ratio, flight speed, and cruise altitude on required thrust power and battery energy and presents the conceptual and preliminary design of a four-seat, general aviation electric aircraft with a takeoff weight of 1750 kg, a range of 800 km, and a cruise speed of 200 km/hr. An innovative configuration design will take full advantage of the electric propulsion system, while a Lithium-Polymer battery and a DC brushless motor will provide the power. Advanced aerodynamics will explore the greatest possible extend of laminar flow on the fuselage, the wing, and the empennage surfaces, to minimize drag, while advanced composite structures will provide the greatest possible savings on empty weight. It is intended for the proposed design to be certifiable under current FAR 23 requirements.**

*Keywords – electric aircraft, batteries, energy density, lift-to-drag ratio,laminar flow, FAR 23.*

## I. INTRODUCTION

It is now recognized that emission of carbon, nitrogen oxides, halogens, and other products from the burning of aviation fuel contributes to the climatic change we have been experiencing (e.g. ozone layer depletion, air quality degradation) [1]. Furthermore, current airplane engines are noisy. The environmental effects of aviation are depicted in Figure 1 [2]. According to GAO Report 2008, aviation emissions contribute about 1% of the air pollution and 2.7% of the US green house gas emissions. Although these percentages seem small, the global air traffic is predicted to increase at a rate of 20% by 2015 and 60% by 2030. Currently, global aircraft emissions produce about 3.5% of the warming generated by human activity [2]. However, if unchecked, by 2021 the emissions may increase up to 90% from the current level [2].
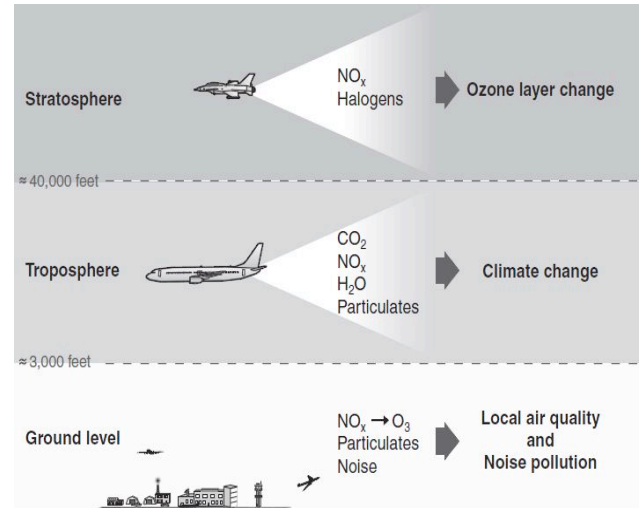


Figure 1. Environmental effect of aviation emission and noise [2].

This negative impact on our environment can be reduced by introducing more eco-friendly propulsion systems and suitable airplane desings and this is where elctric aircraft have a very important role to play.

Figure 2.   Effect of climate change and its consequence.



Figure 3.   Growth in aviation related pollutants by 2021.

## II.      THE ROLE OF ELECTRIC AIRCRAFT

The advantages of electric motors (EM) compared to biofuel are summarized below [3 – 5].

- Very light weight  (45 lbs for EM, compared to 400 lbs for ICE)
- More power per unit weight
- More efficient energy conversion (90-95% for EM, compared to 20-25% for ICE)
- Improved high altitude performance (higher ceiling as well as airspeed and climb rate)
- Noise reduction
- High reliability and safety
- Lower operating cost  ($5-$10/hr for EM, compared to $35-$50/hr for ICE)
- Easier maintenance
- Low pollution

## III.      EXISTING DESIGNS

### A.  Existing Electric Aircraft Designs

Tables 1 and 2 summarize data on the propulsion types of electric aircraft [6 – 9]. Table 1 refers to existing aircraft, while Table 2 presents data on aircraft currently under research.

TABLE 1 – EXISTING ELECTRIC AIRCRAFT

| Company | Name | Type | Propulsion |
|---|---|---|---|
| PC AERO | Electra One | 1 - Seat | Electric Motor + Li Po Battery |
| YUNEEC | E 430 | 2 - Seat | Electric Motor + Li Po Battery |
| EADS | Cri-Cri | 1 – Seat | Electric Motor + Li Po Battery |
| PIPISTREL | Taurus Electro G2 | 2 – Seat | Electric Motor |
| BOEING | ------- | 1 – Seat | Electric Motor |
| SIKORSKY | Firefly | Helicopter | Electric Motor |
| PIPISTREL | Panthera | 4 - Seat | |

TABLE 2 – ELECTRIC AIRCRAFT UNDER RESEARCH

| Company | Name | Type | Propulsion |
|---|---|---|---|
| LANGE AVIATION | Antares 3 | UAV | Electric Motor + Fuel Cell |
| YUNEEC | E 1000 | 4-Seat | Electric Motor + Li Po Battery |
| FLIGHT DESIGN | ------ | 4-Seat | Electric Motor + ICE |
| BYE ENERGY | ------ | 2-Seat | Electric Motor + APU |

## IV.      DESIGN REQUIREMENTS

The design requirements for the proposed aircraft are as follows.

- General aviation, FAR 23 certifiable
- 4 passengers (including pilot)
- Electrically powered
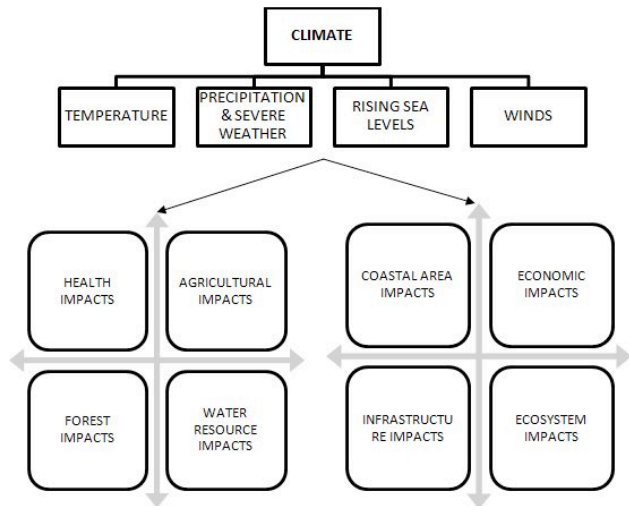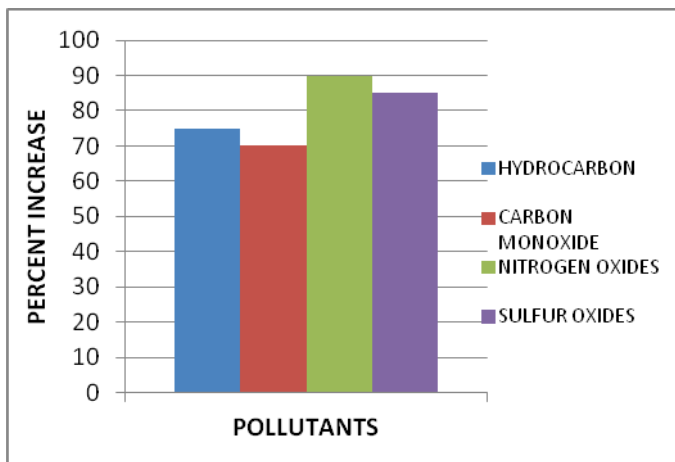- Range = 800 km
- Cruise speed = 200 km / hr

# V.  PROPULSION TYPE SELECTION

The following factors are taken into consideration in the selection of the propulsion system:

1. Power density
2. Energy density
3. Safety
4. Cost
5. Reliability

A trade study was performed to decide the type of energy source, namely a battery or a fuel cell. The battery and fuel cell characteristics needed to produce 135 hp in a ground based electric vehicle are shown in Tables 3 and 4 [13]. Based on this comparison, the best option is the battery due to its lower weight, volume, and cost. Although the energy density of the fuel cell is higher than that of the battery, the space occupied by the fuel cell is too large to be used in a 4 seat aircraft.

TABLE 3 – FUEL CELL SPECIFICATIONS

| Component | Weight (Kg) | Volume (Liters) | Cost ($) |
|---|---|---|---|
| Fuel Tank | 617 | 1182 | 23,033 |
| 3.2 kg Storage Tank | 51 | 215 | 2,288 |
| Drive Train | 53 | 68 | 3,826 |
| TOTAL | 721 | 1465 | 29,147 |

TABLE 4 – BATTERY SPECIFICATIONS

| Component | Weight (Kg) | Volume (Liters) | Cost ($) |
|---|---|---|---|
| Li ion Battery | 451 | 401 | 16,125 |
| Drive Train | 53 | 68 | 3,826 |
| TOTAL | 504 | 469 | 19,951 |

The following sections explain the characteristics of motor and battery selection. The lightest and most efficient devices have been chosen for the proposed design.

## A.  Electric Motor Characteristics

A DC brushless motor is chosen because of its higher reliability and higher torque at lower rpm. The brushless motor is a purely inductive. Unlike a brushed motor, there is no brush to replace, so the motor life depends mostly on the bearings.

## B.  Propeller Characteristics

The desired characteristics of the propeller are to have the lightest possible weight, and to produce the lowest possible noise for the desired level of thrust.

Increasing the number of blades decreases noise, but it also increases the structural weight and decreases blade efficiency, as each blade rotates in the wake of a closely positioned blade. Decreasing the number of blades, on the other hand, requires a larger diameter for the propeller, which increases noise, as the propeller tip rotates at higher speeds and reduces the ground clearance. Based on these considerations, a propeller with three blades was chosen for our proposed design.

The diameter of the propeller is obtained from the following equation [10]:

$$D_p = \left(\frac{4P_{max}}{\Pi n_p P_{bl}}\right)^{0.5} \tag{1}$$

where

$P_{bl}$ - power loading per blade hp/ft$^2$

$n_p$ - number of blades

$P_{max}$ - maximum engine power hp

$P_{bl} = 3.2$

$P_{max} = 203.5\ HP$

$n_p = 3$

$D_p = 5.2\ ft$

## C.  Battery Characteristics

The battery source is selected based on the specific energy, specific power and operating voltage range of the battery. Table 5 shows different battery types. Based on tis comparison, the Li-Po battery seems to offer all of the desirable characteristics for our proposed airplane [14].

TABLE 5 – COMPARISON OF DIFFERENT BATTERIES

| Battery | Theoretical Specific Energy (W-hr/kg) | Practical Specific Energy(W-hr/kg) | Specific Power(W/kg) | Cell Voltage(V) |
|---|---|---|---|---|
| Pb/acid | 170 | 50 | 180 | 1.2 |
| Ni/Cd | 240 | 60 | 150 | 1.2 |
| NiMH | 470 | 85 | 400 | 1.2 |
| Li-ion | 700 | 135 | 340 | 3.6 |
| Li-Po | 735 | 220 | 1900 | 3.7 |
| LiS | 2550 | 350 | 700 | 2.5 |

## VI. PRELIMINARY SIZING

The preliminary sizing of the aircraft is performed following the steps in reference [10].

### A. Takeoff Weight Estimation

The takeoff weight is subdivided into different groups as shown below. A general idea of the weight of each group is obtained from existing electric aircraft, such as the Taurus G4, the Diamond DA40, and the Cessna Corvalis TTX.

$$W_{TO} = W_E + W_P + W_B + W_{PL} \qquad (2)$$

$W_{TO}$ = Takeoff weight
$W_E$ = Empty weight (structures, avionics, etc.)
$W_P$ = Propulsion system weight (propeller, motor, motor controller)

$W_B$ = Battery weight

$W_{PL}$ = Payload

Using data from existing electric aircraft for guidance, these weights are estimated as follows:

$W_E$ = 750 kg
$W_P$ = 100 kg
$W_{PL}$ = 400 kg (each passenger: 75 kg + 25 kg for luggage)
$W_B$ = 500 kg

Hence,   $W_{TO}$ = 1750 kg.

The design point is obtained from the performance sizing graph. The aircraft is sized according to the FAR 23 requirements.
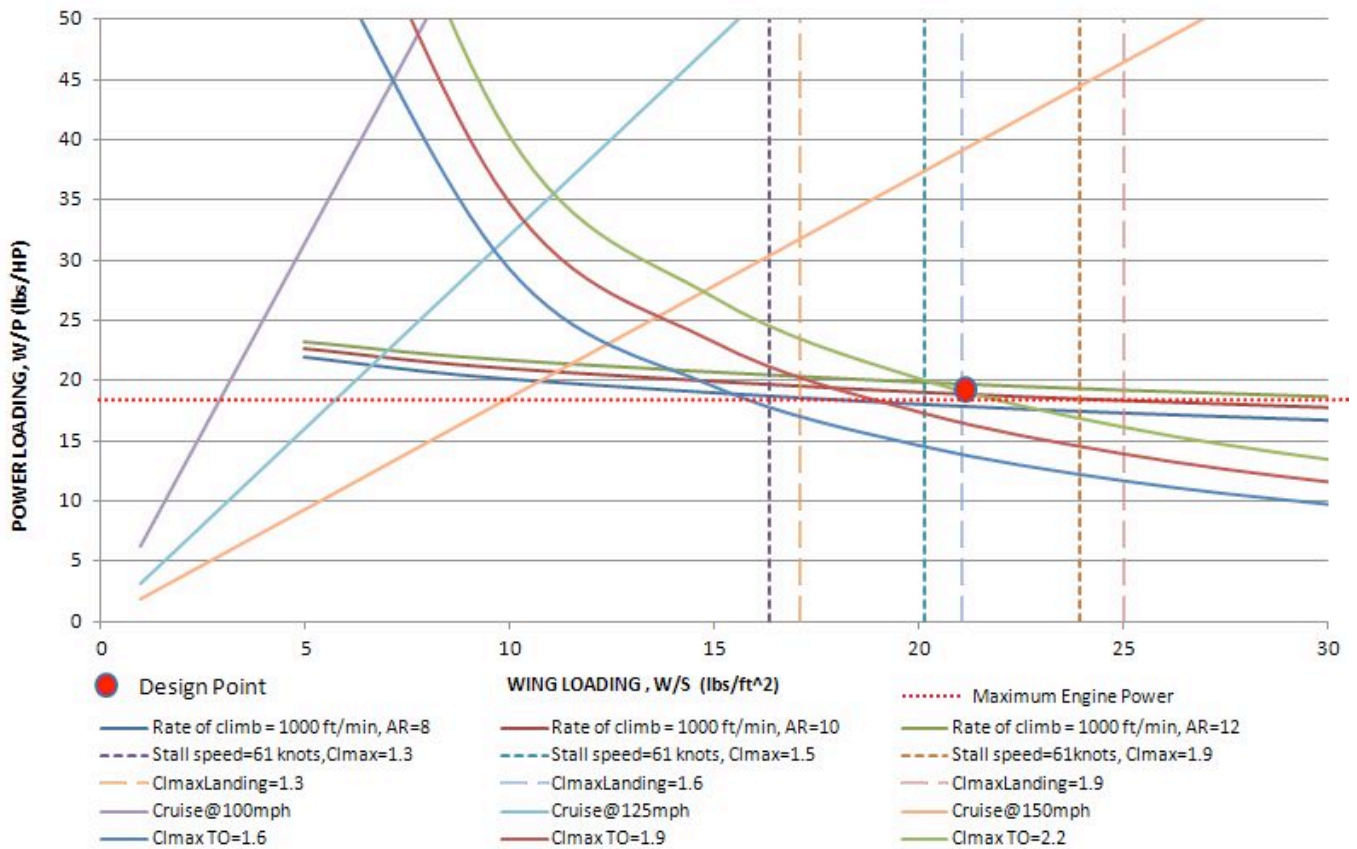


Figure 4. Performance sizing graph.

## B. Summary of Performance Sizing

The design point chosen is shown on the performance sizing graph. Table 6 provides the summary of .

TABLE 6. SUMMARY OF PERFORMANCE SIZING

| | |
|---|---|
| Stall Speed | 61 Knots |
| Rate of Climb | 1000 ft/min |
| $C_{l, \max TO}$ | 2.2 |
| $C_{l, \max L}$ | 1.6 |
| Aspect Ratio | 10 |
| Takeoff Wing Loading | 21 lbs / ft$^2$ |
| Takeoff Power Loading | 19 lbs / hp |
| Wing Span | 43 ft |
| Chord | 4.3 m |
| Engine Power | 203 hp |

## C. Battery Sizing

The battery is sized following the method in reference [14]. The thrust power generated by the propeller is:

$$P_{Thrust} = T \cdot V \tag{3}$$

For level, unaccelerated flight, thrust equals drag. Hence,

$$P_{Thrust} = D \cdot V = \frac{W_{TO}}{\frac{L}{D}} \cdot V \tag{4}$$

The energy needed from the battery is:

$$E = \frac{E_B}{P_B} \tag{5}$$

where,

E = Endurance of flight
$E_B$ = Battery Energy
$P_B$ = Battery Power
$1 \, KWH = 3.6 * 10^6 \, J$

The specific energy (KWh) is found out using the above conversion method. The mass of the battery is estimated using the specific energy of Li-Po battery. Tables 6 and 7 show the thrust power, specific energy and battery mass battery required for different L/D ratios and cruise velocities. The endurance changes as a function of cruise speed. A 30-minute reserve has been taken into account. The mass of the battery is calculated based on the theoretical specific energy of the battery.

TABLE 7. EFFECT OF L/D OVER THRUST POWER AND BATTERY ENERGY

| L/D | Thrust Power(KW) | | | Battery Energy(MJ) | | |
|---|---|---|---|---|---|---|
| | *V=150Km/hr* | *V=200Km/hr* | *V=250Km/hr* | *V=150 Km/hr* | *V=200Km/hr* | *V=250Km/hr* |
| 13 | 73 | 96.9 | 121.2 | 1525.6 | 1570.1 | 1613.7 |
| 14 | 67.5 | 90 | 112.5 | 1416.7 | 1458 | 1498.5 |
| 15 | 63 | 84 | 105 | 1322.2 | 1360.8 | 1398.6 |
| 16 | 59 | 78.7 | 98.4 | 1239.6 | 1275.7 | 1311.1 |
| 17 | 55.6 | 74.1 | 92.6 | 1166.7 | 1200.7 | 1234.1 |
| 18 | 52.5 | 70 | 87.5 | 1101.8 | 1134 | 1165.5 |
| 19 | 49.7 | 66.3 | 82.8 | 1043.8 | 1074.3 | 1104.1 |
| 20 | 47.3 | 63 | 78.7 | 991.6 | 1020.6 | 1048.9 |
| 21 | 45 | 60 | 75 | 944.4 | 972 | 999 |
| 22 | 42.9 | 57.3 | 71.6 | 901.5 | 927.8 | 953.5 |
| 23 | 41.1 | 54.8 | 68.5 | 862.3 | 887.4 | 912.1 |
| 24 | 39.4 | 52.5 | 65.6 | 826.4 | 850.5 | 874.1 |
| 25 | 37.8 | 50.4 | 63 | 793.3 | 816.4 | 839.1 |

TABLE 8. EFFECT OF L/D OVER SPECIFIC ENERGY AND BATTERY MASS

| L/D | Specific Energy(KW-hr) | | | Battery Mass (Kg) | | |
|---|---|---|---|---|---|---|
| | *V=150Km/hr* | *V=200Km/hr* | *V=250Km/hr* | *V=150 Km/hr* | *V=200Km/hr* | *V=250Km/hr* |
| 13 | 423.7 | 436.1 | 448.2 | 576.5 | 593.4 | 609.8 |
| 14 | 393.5 | 405 | 416.2 | 535.4 | 551.1 | 566.3 |
| 15 | 367.2 | 378 | 388.5 | 499.7 | 514.3 | 528.5 |
| 16 | 344.3 | 354.3 | 364.2 | 468.4 | 482.1 | 495.5 |
| 17 | 324.1 | 333.5 | 342.7 | 440.9 | 453.7 | 466.3 |
| 18 | 306.1 | 315 | 323.7 | 416.4 | **428.5** | 440.4 |
| 19 | 289.9 | 298.4 | 306.7 | 394.5 | 406.1 | 417.3 |
| 20 | 275.4 | 283.5 | 291.3 | 374.7 | 385.7 | 396.4 |
| 21 | 262.3 | 270 | 277.5 | 356.9 | 367.3 | 377.5 |
| 22 | 250.4 | 257.7 | 264.8 | 340.7 | 350.6 | 360.4 |
| 23 | 239.5 | 246.5 | 253.3 | 325.9 | 335.4 | 344.7 |
| 24 | 229.5 | 236.2 | 242.8 | 312.3 | 321.4 | 330.5 |
| 25 | 220.3 | 226.8 | 233.1 | 299.8 | 308.5 | 317.1 |

It is clear from Table 8 that a L/D ratio of 16 or above is required at a cruise velocity of 200 km/hr to achieve a battery mass of no more than 500 kg, as estimated in the preliminary weight sizing earlier.

## VIII.  PRELIMINARY DESIGN

### A.  Fuselage Layout

The fuselage is sized to provide adequate space for four passengers and their baggage. The method in reference [10] is used to decide on the values of the various fuselage parameters.
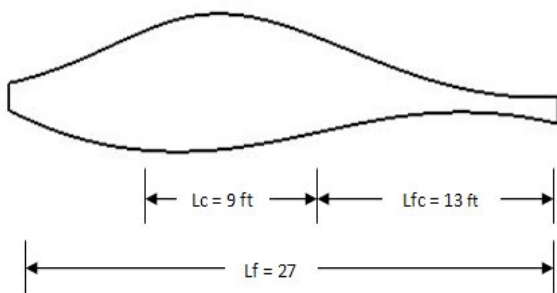


Figure 5.    Fuselage side view.



Figure 6.    Fuselage front view.

Fuselage Diameter = 4.5 ft
Fuselage Length = 27 ft
Tail Cone Length = 13.5 ft
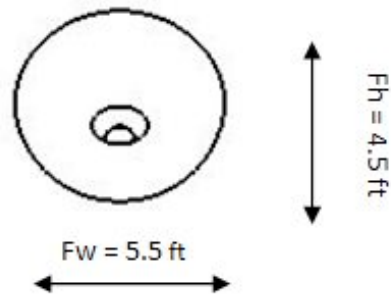
Cabin Dimensions:
Maximum Height = 4.5 ft
Maximum Width = 5.5 ft
Maximum Length = 9 ft

## B. Engine Selection And Disposition

To provide a clean flow over the wings, a fuselage mounted single engine is chosen. An electric motor with an output power of 160 KW and a 3-blade propeller with a diameter of 5.2 ft are selected. The engine location is shown in Figure 7.
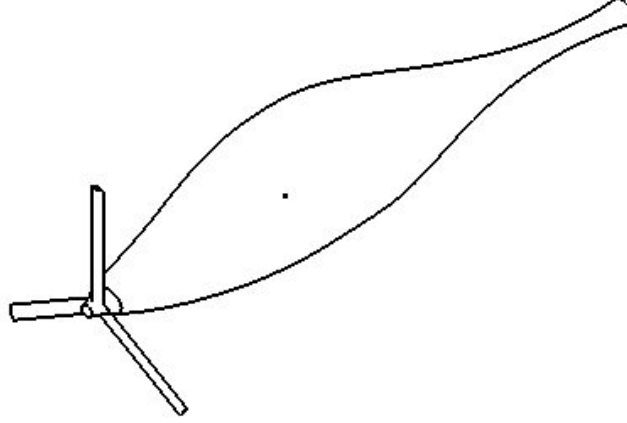


Figure 7. Nose mounted engine.

## C. Wing Design

A cantilever, low wing is selected for the design due to its favorable ground effect during takeoff and the shorter landing gear, which helps in reducing the structural weight. Also, the wings can be used as a step to enter into the aircraft. From the summary of the performance sizing results, the wing specifications can be calculated:

$S = 184$ ft$^2$
$AR = 10$
$b = 43$ ft
$c = 4.3$ ft

From the existing data of similar aircraft using [10], the other wing parameters such as taper ratio, dihedral angle, sweep angle and twist angle and incidence angle are also obtained.

Taper ratio = 0.4
Dihedral = 7°
Sweep = 0°
Wing twist = -3°
Incidence angle = 2°

From reference [13],

$$\bar{c} = \frac{2}{3} C_r \left( \frac{1 + \lambda + \lambda^2}{1 + \lambda} \right) \quad (6)$$

where,

$\bar{c}$ = mean aerodynamic chord = 4.3 ft
$\lambda$ = taper ratio = 0.4
$c_r$ = root chord = 5.78 ft
$c_t$ = 2.31 ft

To find the flap dimensions, the following approximation is used:

$c_f / c = 0.2$
$b_f / b = 0.7$

Hence, the flap dimensions are:
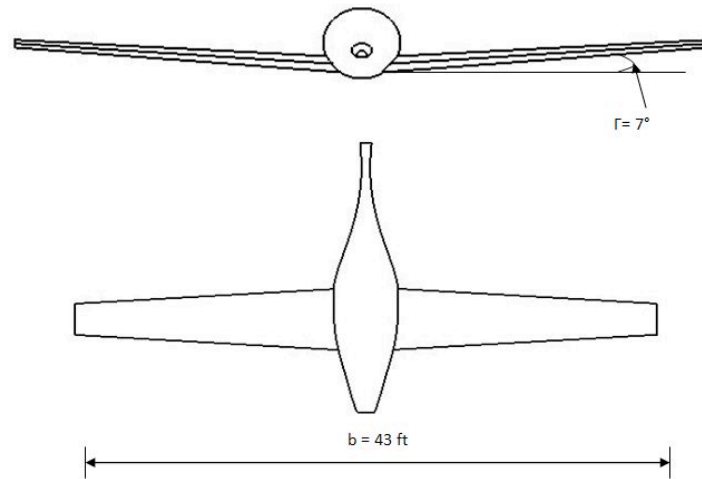
$c_f = 0.86$ ft
$b_f = 30$ ft

Figure 8.    Wing specifications.

## D.  *Weight and Balance Analysis*

The various components that contribute to the aircraft weight are shown in Figure 9 for the purpose of estimating the aircraft cg.  Table 9 shows an estimation of the empty weight cg, while Table 10, using data from existing aircraft [10], gives the location of the aircraft cg at 10 ft from the nose of the fuselage.

TABLE 9.  ESTIMATION OF EMPTY WEIGHT CG

| Component | Weight (kg) | X (m) |
|---|---|---|
| Wings | 265 | 2.56 |
| Empennage | 65 | 7.62 |
| Fuselage | 250 | 2.46 |
| Nose Landing Gear | 20 | 1.83 |
| Main Landing Gear | 100 | 2.54 |



1 - Motor + Controller
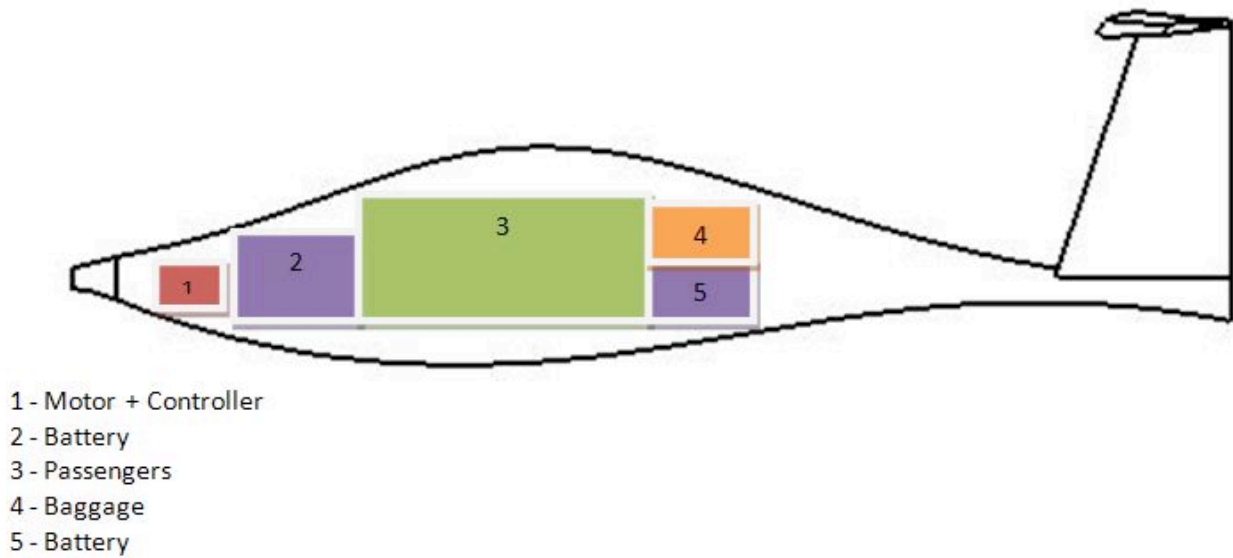2 - Battery
3 - Passengers
4 - Baggage
5 - Battery

Figure 9.  Location of various components for the purpose of estimating the cg location.

TABLE 10.   CG ESTIMATION

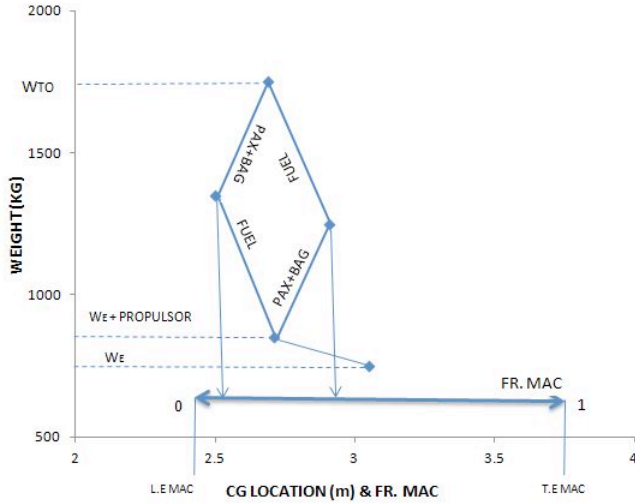| Component | Weight (kg) | x (m) |
|----------|-------------|-------|
| Propulsor Unit | 100 | 0.15 |
| Battery | 350 | 1.06 |
| Passengers | 300 | 2.89 |
| Empty Weight | 750 | 3.04 |
| Baggage | 100 | 4.72 |
| Battery | 150 | 4.72 |



Figure 10.   CG excursion diagram.

From Figure 10, the cg travel of the aircraft is 16 in or 31% of the wing mean aerodynamic chord.

*E.   Landing Gear*

A retractable, conventional, tricycle landing gear is chosen to reduce drag and to provide the greatest extent of laminar flow over the wing during cruise. The landing gear specifications and location are determined by the ground clearance and tip over criteria [10].  To provide adequate clearance for the propeller, the length of the nose landing gear is chosen at 4 ft and the length of the main landing gear at 3 ft.

The nose gear is placed 86 inches from the nose of the fuselage, while the main gear is located 125 inches of the fuselage section. The static load per strut for the nose and main landing gears is found from:

$$\frac{P_n}{W_{to}} = 0.25$$

$$\frac{2P_m}{W_{to}} = 0.74$$

(7)

From equation (7) and typical landing gear wheel data [10], the landing gear specifications are easily obtained.

*F.   Empennage*

A T–tail is chosen for the proposed design because it provides the best location for staying out of the wing wake and it increases the efficiency of the horizontal stabilizer, requiring thus a smaller area.   From the configuration layout, the distance of the horizontal and the vertical stabilizer from the cg are obtained:

$X_h$ = 15 ft,          $X_v$ = 14.5 ft

Hence

$S_h$ = 32.2 ft$^2$,      $S_v$ = 20.2 ft$^2$
$b_h$ = 12.7 ft,      $b_v$ = 30.3 ft
$c_h$ = 2.54 ft;      $c_v$ = 3.7 ft

A taper ratio of 0.5 is chosen on both the horizontal and the vertical stabilizers based on data from similar aircraft [10].

*G.   High Lift Devices*

Figure 11 shows different high lift devices, while Table 11 gives the increment in lift coefficient for each device [13].



a.   Plain flap
b.   Split flap
c.   Single slotted flap
d.   Double slotted flap
e.   Triple slotted flap
f.   Fowler flap
**a.**  *Trailing edge high lift device*

g.   Leading edge flap
h.   Leading edge slat
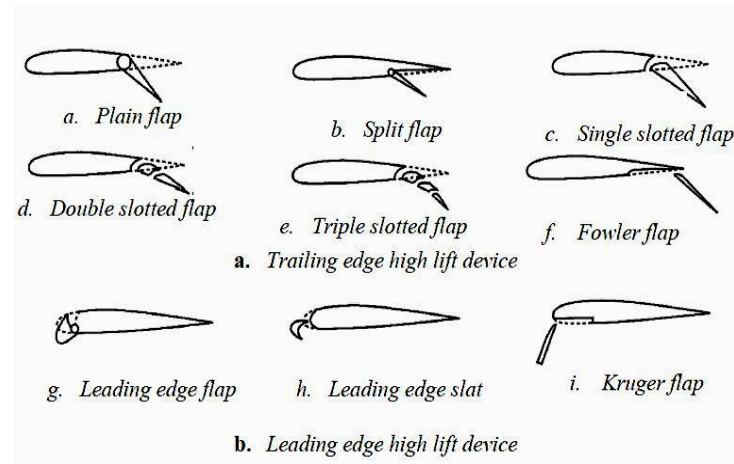i.   Kruger flap
**b.**  *Leading edge high lift device*

Figure 11.  High lift devices.

A plain flap is the most simple high lift device which provides a maximum increment of 0.9 while adding less structural weight. Hence a plain flap is chosen in this design.

TABLE 11.  LIFT COEFFICIENT INCREMENTS
FOR VARIOUS TYPES OF HIGH LIFT DEVICES

| HIGH LIFT DEVICE | ΔCl |
|------------------|-----|
| Plain Flap | 0.7-0.9 |
| Split Flap | 0.7-0.9 |

| | |
|---|---|
| Fowler Flap | 1-1.3 |
| Slotted Flap | 1.3 Cf/C |
| Double Slotted Flap | 1.6 Cf/C |
| Triple Slotted Flap | 1.9 Cf/C |
| Leading Edge Flap | 0.2-0.3 |
| Leading Edge Slat | 0.3-0.4 |
| Kruger Flap | 0.3-0.4 |

*H. Airfoil Selection*

The ideal and maximum lift coefficients for the airfoil are calculated from the equations in reference [13]:

$C_{lideal} = 0.8$
$C_{lmax} = 1.4$

The airfoil is chosen primarily based on these two criteria. The ideal lift coefficient is higher when compared to the average ideal lift coefficient, which is usually in the range of 0.2 – 0.4. Hence, the induced drag produced by the wing will be higher, but the Pipistrel Panthera has an ideal lift coefficient of 0.7, which is comparable. The airfoils that have the highest ideal lift coefficient are considered to find the best suitable one.

The NACA 6-series airfoils have high ideal lift coefficient [13]. A number of airfoils were selected and their lift, drag, and pitching moment characteristics are compared in Figures 12 through 17, to find the best airfoil. From the results, two airfoils, NACA 65618 and NACA 66212 were selected and compared. The NACA 65618 generated high lift-to-drag ratios during cruise and a smaller pitching moment coefficient, hence it was chosen for our proposed design.
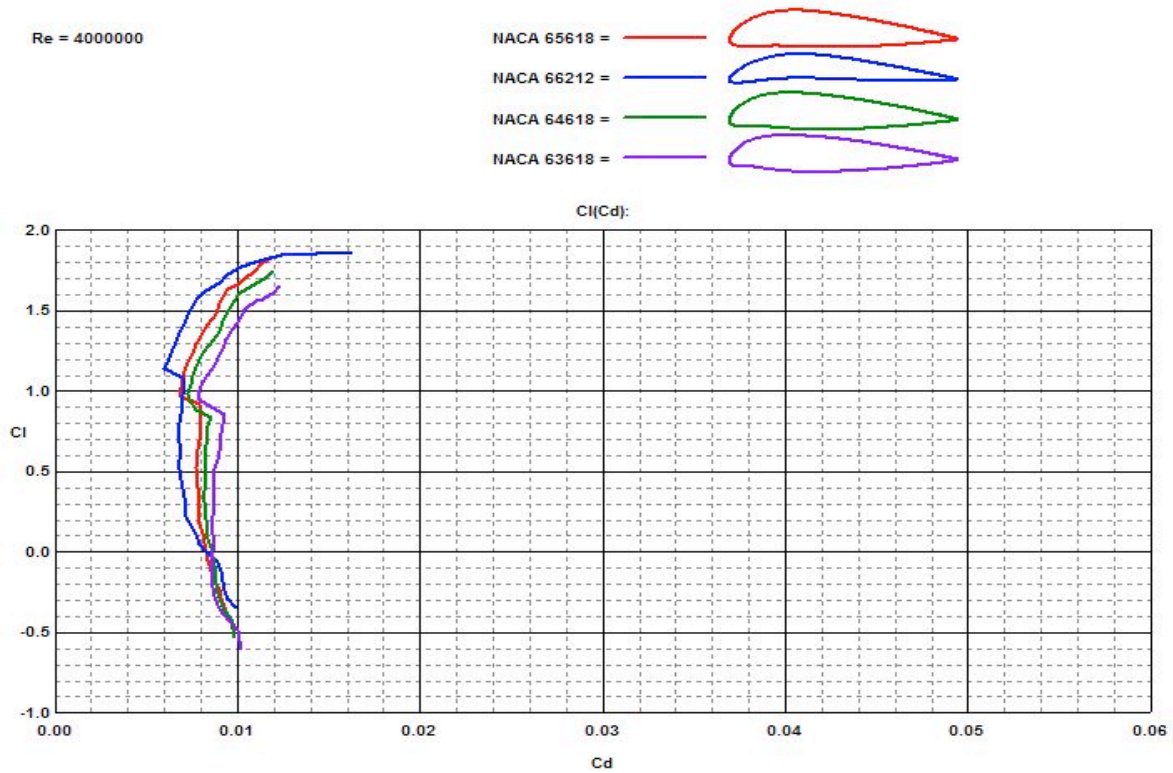


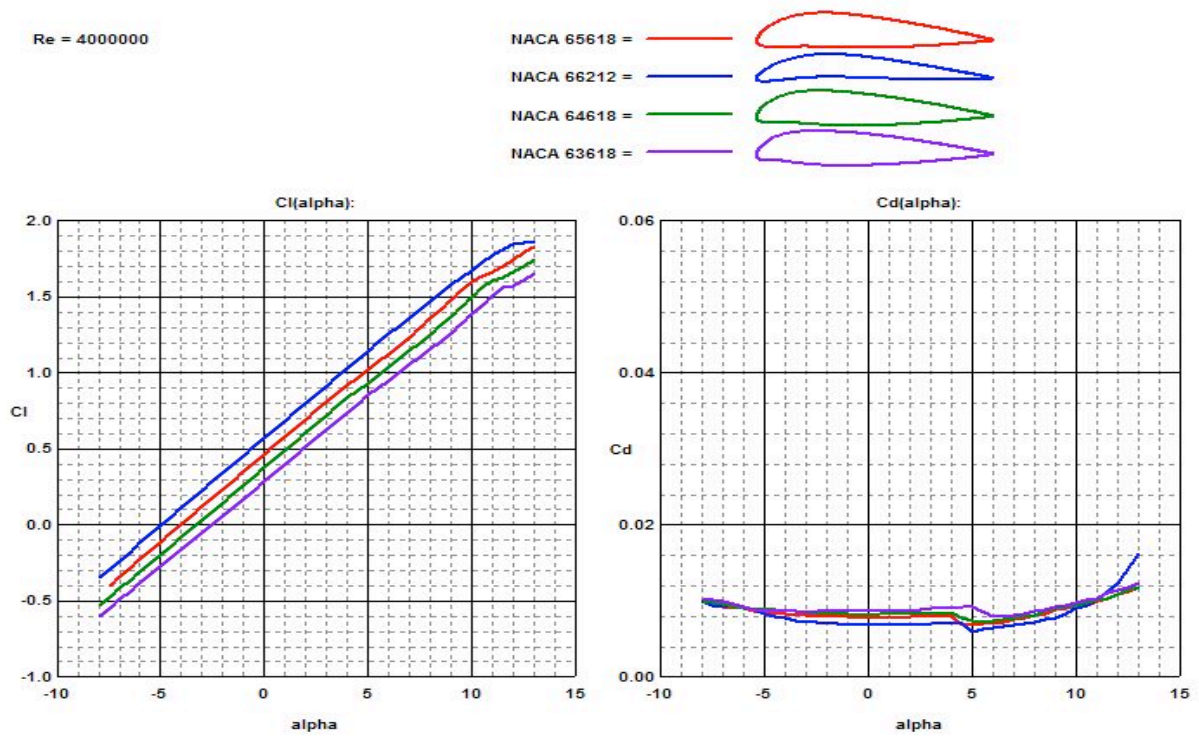Figure 12.  Drag polar comparison of various NACA 6-series airfoils.

Figure 13.   Lift and drag characteristics comparison of various NACA 6-series airfoils.
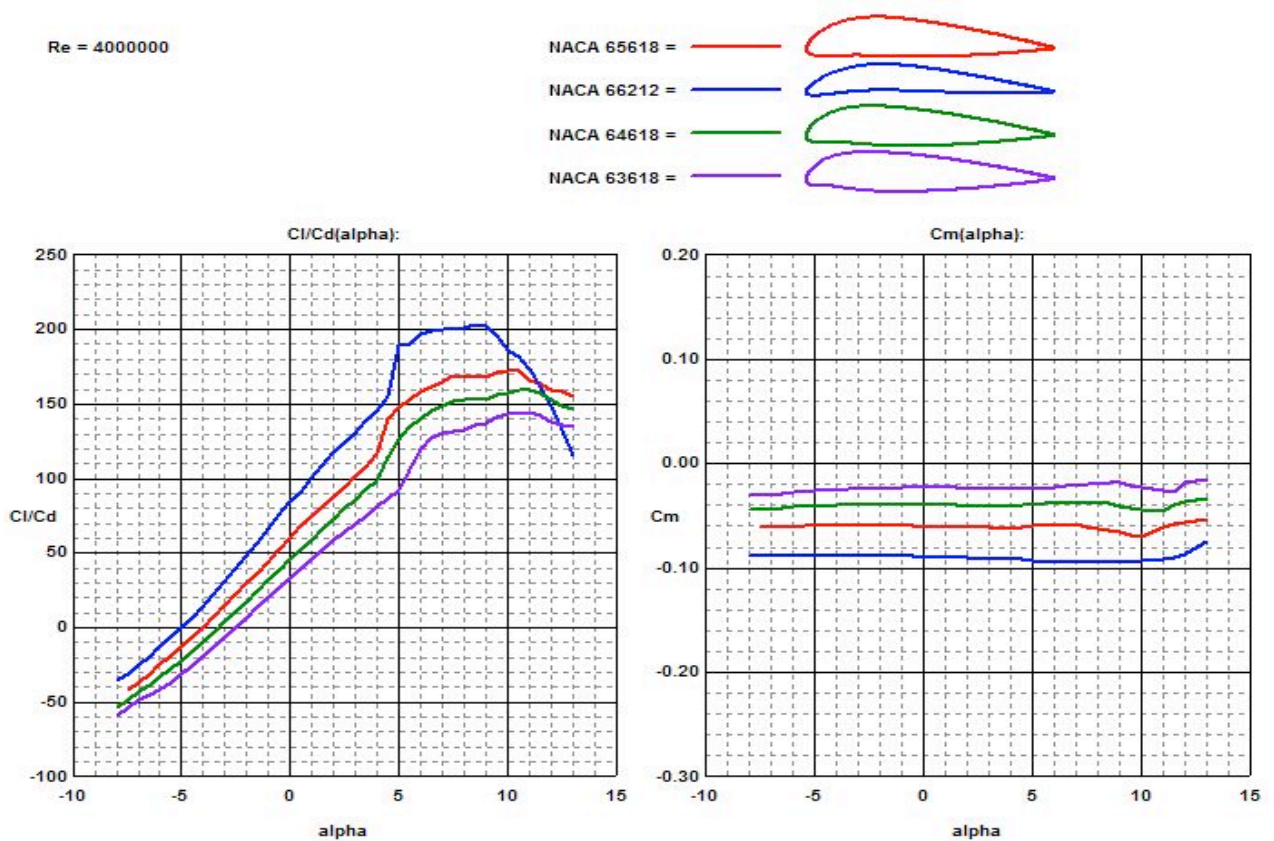


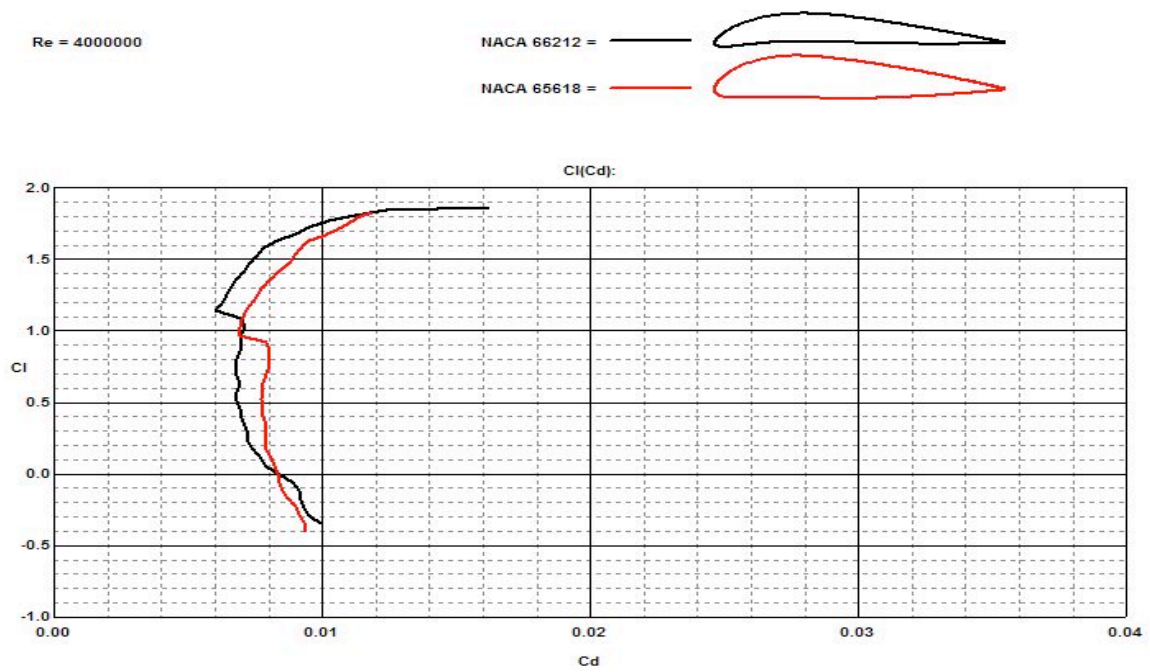Figure 14.  Lift-to-drag ratio and pitching moment comparison of various NACA 6-series airfoils.

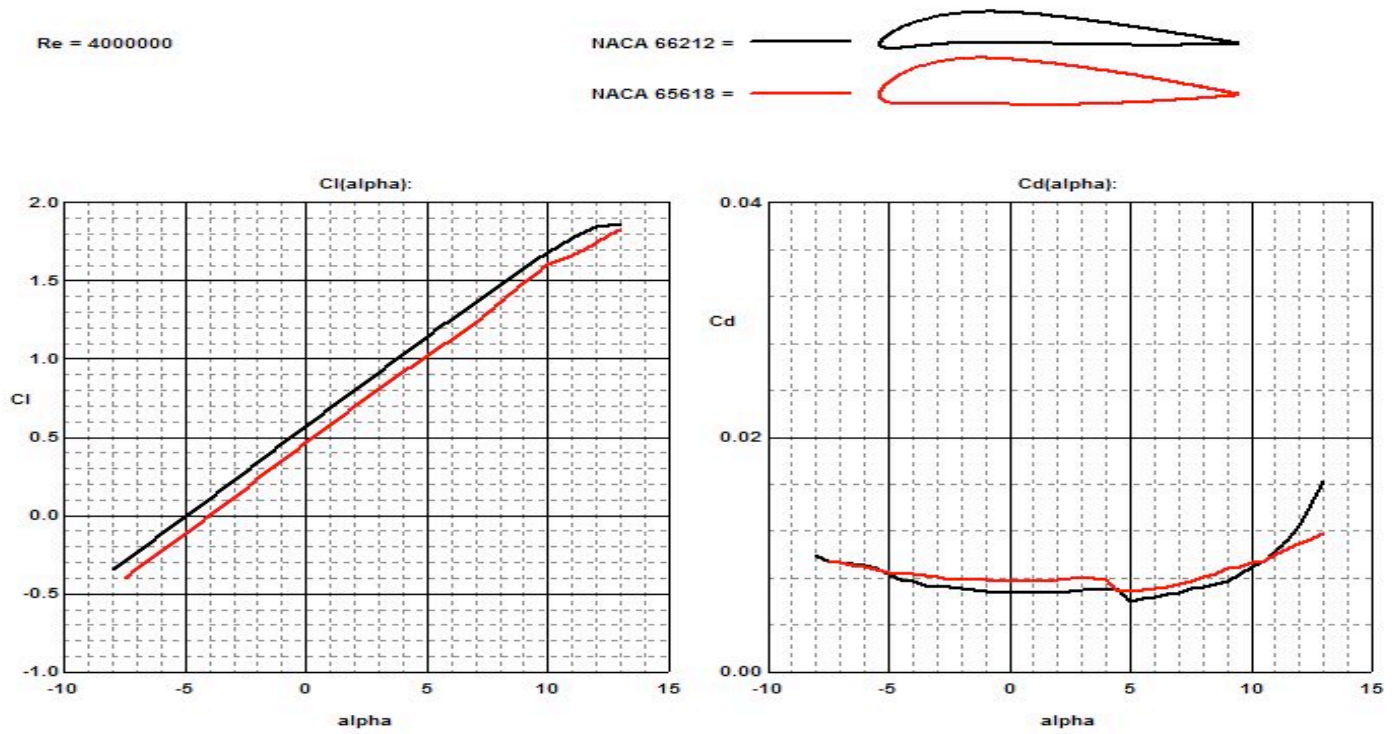Figure 15. Comparison of the drag polars for the NACA 66212 and NACA 65618 airfoils.



Figure 16. Comparison of the lift and drag characteristics of the NACA 66212 and NACA 65618 airfoils.
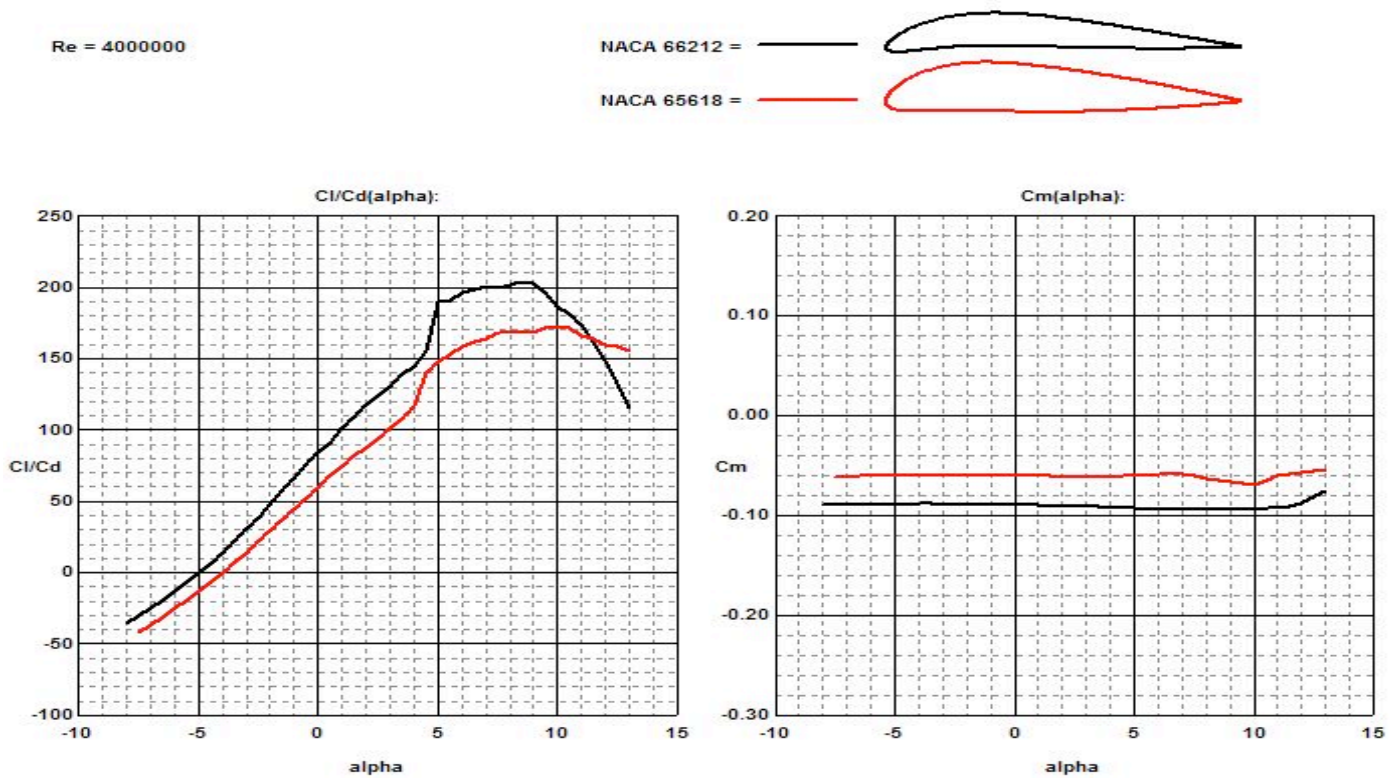
Figure 17. Comparison of the lift-to-drag ratio and pitching moment of the NACA 66212 and NACA 65618 airfoils.

## I. DRAG POLAR

The preliminary estimates of the airplane low-speed drag coefficient and Oswald efficiency factor are estimated for different configurations of the aircraft and shown in Table 12 [10].

$$C_{D_0} = 0.02$$

$$C_D = C_{D_0} + \frac{C_l^2}{\Pi A e} \tag{9}$$

TABLE 12. PRELIMINARY ESTIMATES OF $C_{do}$ AND $e$

| Configuration | $C_{D_0}$ | E |
|---|---|---|
| Clean | 0 | 0.80-0.85 |
| Takeoff Flaps | 0.010-0.020 | 0.75-0.80 |
| Landing Flaps | 0.055-0.075 | 0.70-0.75 |
| Landing gear | 0.015-0.025 | No effect |

TABLE 13. DRAG COEFFICIENT AND LIFT-TO-DRAG RATIO FOR DIFFERENT AIRCRAFT CONFIGURATIONS

| Configuration | $C_D$ | $C_l$ | L/D |
|---|---|---|---|
| Clean | 0.044 | 0.8 | 18 |
| Take off, gear up | 0.22 | 2.2 | 10 |
| Takeoff, gear down | 0.24 | 2.2 | 9 |
| Landing, gear up | 0.18 | 1.6 | 8.7 |
| Landing, gear down | 0.19 | 1.6 | 8 |

The wetted surface area of the aircraft is estimated to be $S_{wet} = 676$ ft$^2$, while the equivalent parasite area is estimated at f = 4. Hence:

$$C_{D_0} = \frac{f}{S} \tag{8}$$

$$\left(\frac{L}{D}\right)_{max} = 18$$

13

This value for $(L/D)_{max}$ obtained from our drag polar satisfies the initial estimate of the battery mass, as shown earlier in Table 8, hence, no iteration is needed.

## J. PRELIMINARY DESIGN LAYOUT

Figure 18 shows the preliminary design layout of the proposed 4-seat, general aviation, electric aircraft.
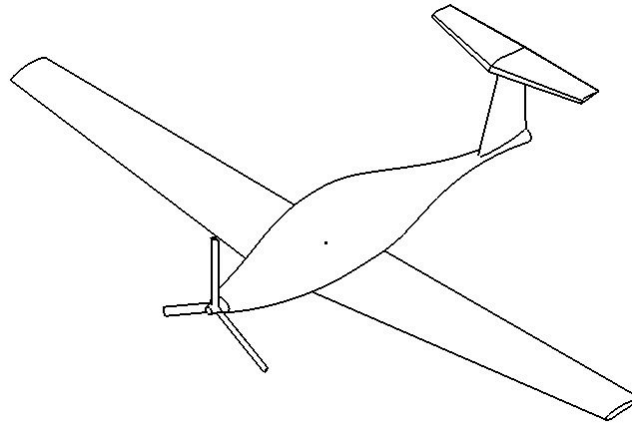


Figure 18. Preliminary design layout.

It is noted that the range and efficiency of the electric aircraft depends heavily on the takeoff weight. The takeoff weight of 1,750 kg is much higher when compared to aircraft of the same category, such as, fo example, the Pipistrel Panthera, which has a takeoff weight of 1,200 kg. This, of course, is due to the higher L/D ratio, which reduces the energy needed during flight, and as a consequence, the required battery weight. Needless to say, the proposed design extrapolates on advances in battery technology, composite structures, and aerodynamics to help achieve the performance shown in this paper. The next step is a detailed analysis of each subsystem to confirm the feasibility of the proposed concept.

## REFERENCES

[1]  A. Epstein, Aircraft propulsion, presented at NASA ARC green aviation workshop, Mountain View, April 2009.

[2]  G.L. Dillingham, Aviation and the Environment, United States Government Accountability Office, 2008.

[3]  CAFE: Electric aircraft symposium report, 2010. Viewed at <http://www.youtube.com/watch?feature=endscreen&NR=1&v=d24knbykgVo>

[4]  Aero-tv: Bye energ'ys electric 172 - building a greener future for aviation, 2011. Viewed at <http://www.youtube.com/watch?v=Yjq8ixM0oEw>

[5]  D. Yoney, Cessna Developing Electric-Powered 172 Skyhawk, 2010. Retrieved from <http://green.autoblog.com/2010/08/11/cessna-developing-electric-powered-172-skyhawk/>

[6]  J. Croft, Electric Propulsion is Gaining Horsepower with Experimental and Light Aircraft Communities, Aug. 02, 2010. Retrieved from <http://www.flightglobal.com/news/articles/electric-propulsion-is-gaining-horsepower-with-experimental-and-light-aircraft-communities-345516>

[7]  R. Coppinger, The Future is Electric for General Aviation, Apr 06, 2010. Retrieved from <http://www.flightglobal.com/news/articles/the-future-is-electric-for-general-aviation-340170>

[8]  Electric Aircraft, Mar. 09, 2012. Retrieved from <http://en.wikipedia.org/wiki/Electirc_aircraft>

[9]  Antares H2/H3 Technical Data. Retrieved from <http://www.lange-aviation.com/htm/english/products/antares_h3/technical_data.html>

[10] J. Roskam, Airplane Design vol I - Preliminary Sizing of Airplanes, 1985.

[11] K. Loftin, Subsonic Aircraft: Evolution and the Matching of Size to Performance. NASA Reference Publication 1060.

[12] M. Sadraey, Aircraft Design: A Systems Engineering Approach. Wiley, 2012.

[13] E. Stephen, E. James, E. A Cost Comparison of Fuel-Cell and Battery Electric Vehicles.

[14] J. Gundlach, Designing unmanned aircraft systems, 2012. Retrieved from <http://arc.aiaa.org/doi/book/10.2514/4.868443>